Perspective Shape-from-Shading by Fast Marching

Ariel Tankus
School of Computer Science
Tel-Aviv University
Tel-Aviv, 69978
arielt@post.tau.ac.il

Nir Sochen
School of Mathematics
Tel-Aviv University
Tel-Aviv, 69978
sochen@post.tau.ac.il

Yehezkel Yeshurun
School of Computer Science
Tel-Aviv University
Tel-Aviv, 69978
hezy@post.tau.ac.il

Abstract

Shape-from-Shading (SfS) is a fundamental problem in Computer Vision. At its basis lies the image irradiance equation. Recently, the authors proposed to base the image irradiance equation on the assumption of perspective projection rather than the common orthographic one. The current paper presents a greatly-improved reconstruction method based on the perspective formulation. The proposed model is solved efficiently via a modification of the Fast Marching method of Kimmel and Sethian. We compare the two versions of the Fast Marching method (orthographic vs. perspective) on medical images. The perspective algorithm outperformed the orthographic one. This shows that the more realistic hypothesis of perspective projection improves reconstruction significantly. The comparison also demonstrates the usability of perspective SfS for real-life applications such as medical endoscopy.

1. Introduction

Recovery of Shape-from-Shading (SfS) is a fundamental problem in Computer Vision. Its goal is to solve the image irradiance equation, which relates the reflectance map to image intensity, in a robust way. As this task is nontrivial, most of the works in the field employ simplifying assumptions. It is particularly common to presuppose that projection of scene points during a photographic process is orthographic. This resulted in low stability of reconstruction algorithms.

Many works in the field of Shape-from-Shading have followed the seminal works of Horn [4], [5], who initiated the subject in the 1970s, and assumed orthographic projection ([2], [6], [7], [3], [26], [16], [15], [25], [8], [1], [13], [21] and many more; see [24] for a survey).

The majority of the few works that did employ the perspective projection have been too restrictive and have not addressed the general problem. [22] and [19] assumed that distance variations between camera and surface could be ignored. [18] employed a deformable model for the SfS problem, so reconstruction took place in 3D space. Thus, during the deformation process, the image point onto which a 3D point was projected changed, and its new location should have been interpolated, resulting in a nonuniform sampling of the image.

Another approach to perspective SfS is piecewise planar modelling of the depth function ([10], [12]). However, orthographic and perspective reflectance maps of a plane are identical (see [20]). Therefore, the two types of projection of a piecewise planar surface differ only at the edges, while fully agree at the interior of faces.

Okatani and Deguchi [11] proposed perspective SfS for reconstruction of endoscopic images. Their lighting model assumes the location of a point light source is identical to that of the camera, so the directions of lighting and projection unite at all points. This model was solved using level sets.

Lately, [23] suggested the use of perspective SfS with the Fast Marching method of [7]. This work approximated surface normals in 3D space using the neighboring pixels of the point under examination. Into these approximations the equations of perspective projection were substituted. This approach suffers two drawbacks. First, is describes a specific numerical approximation without reference to the theoretic problem (i.e., the image irradiance equation itself). Second and most importantly, neighboring pixels lie on a uniform grid (image space), while their 3D correspondents need not be so (in 3D space). The result was that depth derivatives were approximated in 3D space on a nonuniform grid, while the underlying assumption was a uniform one (image space uniformity).

Recently, [20] and [14] suggested the use of a perspective projection model. Both papers introduced the perspective image irradiance equation simultaneously. In [20], the suggested computational algorithm is a very preliminary one, while both algorithms ([20], [14]) are slow and were demonstrated on synthetic images only.

Although the great majority of researches in the field of SfS rely on the orthographic projection, and the minority which applies to perspective SfS is either limited in scope or was used on synthetic examples only, no work employed the image irradiance equation under the perspective projection model for real-life tasks. The goal of this paper is to develop an efficient and robust algorithm for solving the image irradiance equation under the perspective assumption, in a manner that would be adequate for real-life tasks. The proposed solution is a variant of the Fast Marching method of Kimmel and Sethian [7] based on the perspective formulation of the image irradiance equation.

The contribution of this paper will be evaluated by a reconstruction comparison of the proposed algorithm and the original Fast Marching method on medical images from different parts of the gastrointestinal tract (endoscopy). The comparison will show that perspective SfS, in contrast with orthographic SfS (see [24]), should be adequate for real-life applications such as medical endoscopy. We would also see that its runtime is much shorter than required by existing perspective algorithms.

This paper is organized as follows. Following the presentation of notation and basic assumptions (Sect. 2), we review the image irradiance equation under the perspective projection model, and its dependence on the natural logarithm of the depth function (Sect. 3). Section 4 suggests a perspective SfS algorithm based on the Fast Marching method of [7]. Section 5 compares the perspective and orthographic algorithms on medical images. Finally, Sect. 6 draws the conclusions. The Appendix details the generalization of the Fast Marching method to the perspective case.

2. Notation and Assumptions

The following notation and assumptions hold throughout this paper. Photographed surfaces are assumed representable by functions of real-world coordinates as well as of image coordinates. $\hat{z}(x,y)$ denotes the depth function in a real-world Cartesian coordinate system whose origin is at camera plane. If the real-world coordinate $(x, y, \widehat{z}(x,y))$ is projected onto image point (u, v), then its depth is denoted $z(u, v)$. By definition, $z(u, v) = \hat{z}(x,y)$. Pay attention, that $z(u, v)$ is *not* measured along the perspective projection rays, but rather, it relates Cartesian depth ($\hat{z}(x,y)$) to image point (u, v).

f denotes the focal length, and is assumed known. The scene object is Lambertian, and illuminated from a known direction $\vec{L} = (p_s, q_s, -1)$ by a point light source at infinity. $\vec{N}(x, y)$ is the surface normal.

3. The Perspective Image Irradiance Equation

As a first step in solving the image irradiance equation under the perspective projection model, we convert the equation into more convenient forms.

3.1. Equation in Image Coordinates

The perspective image irradiance equation is given by:

$$I(u, v) = \vec{L} \cdot \vec{N}(x, y) \qquad (1)$$

where:

$$x = -\frac{u \cdot \widehat{z}(x,y)}{f} \ , \qquad y = -\frac{v \cdot \widehat{z}(x,y)}{f} \qquad (2)$$

Substituting Eqs. 2 and $\vec{L} = (p_s, q_s, -1)$ (see Sect. 2) into Eq. 1 yields:

$$I(u, v) = \frac{1 + p_s \widehat{z}_x + q_s \widehat{z}_y}{||L||\sqrt{1 + \widehat{z}_x^2 + \widehat{z}_y^2}} \qquad (3)$$

We then express $\widehat{z}_x$ and $\widehat{z}_y$ in terms of u, v, z, z_u, and z_v, and substitute the resultant expressions along with Eqs. 2 into Eq. 3. This yields:

$$I(u, v) = \frac{(u - fp_s)z_u + (v - fq_s)z_v + z}{||L||\sqrt{(uz_u + vz_v + z)^2 + f^2(z_u^2 + z_v^2)}} \qquad (4)$$

where $z(u, v) \overset{def}{=} \widehat{z}(x,y)$ for (u, v) which is the perspective projection of $(x, y, \widehat{z}(x,y))$. Equation 4 is the *perspective image irradiance equation*.

3.2. Dependence on $\ln(z(u, v))$

Equation 4 shows direct dependence on both $z(u, v)$ and its first order derivatives. If one employs $\ln(z(u, v))$ instead of $z(u, v)$ itself (by definition $z(u, v) > 0$), one obtains the following equation:

$$I(u, v) = \frac{(u - fp_s)p + (v - fq_s)q + 1}{||L||\sqrt{(up + vq + 1)^2 + f^2(p^2 + q^2)}} \qquad (5)$$

where $p \overset{def}{=} \frac{z_u}{z} = \frac{\partial \ln z}{\partial u}$ and $q \overset{def}{=} \frac{z_v}{z} = \frac{\partial \ln z}{\partial v}$. Eq. 5 depends on the derivatives of $\ln(z(u, v))$, but not on $\ln(z(u, v))$ itself. Consequently, the problem of recovering $z(u, v)$ from the image irradiance equation reduces to the problem of recovering the surface $\ln(z(u, v))$ from Eq. 5. Because the natural logarithm is a bijective mapping and $z(u, v) > 0$, recovering $\ln(z(u, v))$ is equivalent to recovering $z(u, v) = e^{\ln(z(u,v))}$.

The image irradiance equation under orthographic projection is invariant to translation of $\widehat{z}(x,y)$, which means $\widehat{z}(x,y) + c$ (for constant c) produces the same intensity function as $\widehat{z}(x,y)$. In contrast, the perspective image irradiance equation (Eq. 4) is invariant to scale changes of $z(u, v)$. That is, the intensity functions of $c \cdot z(u, v)$ and $z(u, v)$ are identical. This follows from the properties of the natural logarithm, and can also be verified by Eqs. 4, 5. Invariance to scaling seems to be a more plausible assumption than invariance to translation when employing real cameras.

4. Perspective Fast Marching

This section suggests a perspective SfS algorithm based on the Fast Marching method of Kimmel and Sethian [7].

4.1. Solving the Approximate Problem

The algorithm of Kimmel and Sethian [7] solves the orthographic image irradiance equation $I(x,y) = \vec{L} \cdot \vec{N}(x,y)$. This equation is an Eikonal equation and can be written as:

$$p^2 + q^2 = \tilde{F}^2(x,y)$$

where $p \stackrel{\text{def}}{=} z_u = z_x$, $q \stackrel{\text{def}}{=} z_v = z_y$ and $\tilde{F} = \sqrt{(I(x,y))^{-2} - 1}$. Note, that $\tilde{F}(x,y)$ is independent of p and q. Similarly, the perspective image irradiance equation (Eq. 5), can be transformed into:

$$p^2 A_1 + q^2 B_1 = F \tag{6}$$

where A_1 and B_1 are non-negative and independent of p as well as of q. F, on the other hand, depends on both p and q. The expressions for A_1, B_1 and F appear in Appendix A.

In order to solve an Eikonal equation, we assume that we have estimated $p(u,v)$ and $q(u,v)$ by some process. We use these estimations to derive $F(u,v) = F(p(u,v), q(u,v), u, v)$ and substitute it into the right-hand side of Eq. 6. This results in an Eikonal equation, which we solve for p and q of the left-hand side. We may then use the solution to improve our initial estimation of p and q.

Following [7], we use the numerical approximation:

$$p_{ij} \approx \max\{D_{ij}^{-u}z, -D_{ij}^{+u}z, 0\}$$
$$q_{ij} \approx \max\{D_{ij}^{-v}z, -D_{ij}^{+v}z, 0\}$$

where $D_{ij}^{-u}z = \frac{z_{ij} - z_{i-1,j}}{\Delta u}$ is the standard backward derivative and $D_{ij}^{+u}z = \frac{z_{i+1,j} - z_{ij}}{\Delta u}$, the standard forward derivative in the u-direction ($z_{ij} = z(i\Delta u, j\Delta v)$). $D_{ij}^{-v}z$ and $D_{ij}^{+v}z$ are defined in a similar manner for the v-direction. Rouy and Tourin [17] showed that this numerical approximation selects the correct viscosity solution for the orthographic SfS problem. Substituting into Eq. 6, we get the numerical approximation equation:

$$\left(\max\{D_{ij}^{-u}z, -D_{ij}^{+u}z, 0\}\right)^2 A_1 +$$
$$\left(\max\{D_{ij}^{-v}z, -D_{ij}^{+v}z, 0\}\right)^2 B_1 = F_{ij} \tag{7}$$

where $F_{ij} \stackrel{\text{def}}{=} F(i\Delta u, j\Delta v)$. As Appendix A details, the solution of this equation at every point (i,j) is:

$$z = \begin{cases} z_1 + \sqrt{\frac{F}{A_1}}, & \text{if } z_2 - z_1 > \sqrt{\frac{F}{A_1}} \\ z_2 + \sqrt{\frac{F}{B_1}}, & \text{if } z_1 - z_2 > \sqrt{\frac{F}{B_1}} \\ \frac{A_1 z_1 + B_1 z_2 \pm \sqrt{(A_1+B_1)F - A_1 B_1 (z_1 - z_2)^2}}{A_1 + B_1}, & \text{otherwise} \end{cases} \tag{8}$$

where:

$$z_1 \stackrel{\text{def}}{=} \min\{z_{i-1,j}, z_{i+1,j}\}, \quad z_2 \stackrel{\text{def}}{=} \min\{z_{i,j-1}, z_{i,j+1}\}.$$

4.2. The Iterative Solution

An important observation described in [7] is that information always flows from small to large values at local minimum points. Based on this, the orthographic Fast Marching method reconstructs depth by first setting all z values to the correct height values at local minima and to infinity elsewhere. Then, every step extends reconstruction to higher depths. Reconstruction is thus achieved by a single pass.

Nevertheless, a single pass may not be enough to solve the aforementioned formulation of the perspective problem (Eq. 7), because the approximate solution (the right-hand side of Eq. 8) depends on F, which depends on both p and q. Hence, we suggest an iterative method. For each iteration, F is calculated using the depth recovered at the preceding iteration:

$$p_{n+1}^2 A_1 + q_{n+1}^2 B_1 = F(p_n, q_n)$$

where p_n and q_n are the values of p and q at the nth iteration. Based on this approximation of F and on Eq. 8, a solution is calculated for the new iteration. We initialize this process by the orthographic Fast Marching method of [7].

After each iteration, the resulting depth map was normalized (i.e., divided by the norm of a vector containing all depth values). The reconstruction remains valid after normalization, because perspective SfS is invariant to multiplication by a constant (see Sect. 3.2).

5. Experimental Results

5.1. The Experiments

To evaluate the contribution of perspective SfS, we juxtaposed it with the Fast Marching method [7]. This algorithm was chosen for the comparison for three reasons. First, we consider it a state-of-the-art technique. Second, in [20] we compared three orthographic methods ([9], [26] and [7]) with a basic perspective method that was suggested there. Among the orthographic methods, Fast Marching performed best. Third, because the suggested perspective method is based on Fast Marching, the effect of numerical scheme on results is neutralized. Thus, any improvement would be a consequence of the transition to the perspective equation, and *not* due to different ways of solution.

In contrast with [20], where only synthetic images were compared, this paper experiments with real images solely. We studied endoscopic images of different parts of the gastrointestinal channel.

While endoscopy is a practical field of life on one hand, it has the advantage of a controlled light source environment, on the other hand. The light source can be considered a point light source, but not an infinitely distant one. To overcome this limitation, we worked on a small portion of the original image at a time. This had a double effect. First, it narrowed the range of directions of the light source and second, it limited the range of distances between light source and object. This made the assumption of a constant light source direction plausible, and also diminished the decay of illumination strength with distance.

As postulated in Sect. 2, our theoretic model assumes the light source direction is known. In practice, this kind of information was unavailable, so a human viewer had to produce [very rough] estimations of light source directions from the images themselves (determine azimuth and elevation in multiples of $\frac{\pi}{8}$ or $\frac{\pi}{6}$ radians). The same light source direction was supplied to both orthographic and perspective methods.

In addition, perspective SfS requires the knowledge of the focal length f. Our implementation arbitrarily set an identical value for all examples.

The initialization of the orthographic, and therefore also the perspective, algorithms is based on points of local minima. These were located visually in the photographs by a human viewer. Their depth value was arbitrarily set to the same constant in all images.

For the algorithm of Kimmel and Sethian [7], we extended the implementation of the Fast Marching method by the Technical University of Munich[1] to accommodate the oblique light source case as well. This code served as a basis for implementation of the perspective Fast Marching method too. As a post-processing step, all reconstructions underwent a translation and a rotation to convert camera coordinates to object coordinates, for better visualization.

In our comparison we checked 5 iterations of the perspective Fast Marching for each example (in addition to the orthographic initialization). We found out that all perspective iterations yielded visually-identical images, which implies the suggested algorithm converges very fast. We therefore introduce only the first iteration in this paper.

5.2. Comparative Evaluation

We present in Fig. 1 the comparison between the perspective and orthographic Fast Marching methods. The leftmost column shows the original image, which was cropped to produce the second column. Only the cropped image was used for reconstruction. The third column presents orthographic reconstruction by the Fast Marching method of Kimmel and Sethian [7], while the last column shows reconstruction by the proposed perspective variant after 1 iteration. Each row presents an example from a different part of the gastrointestinal channel.

The top row of Fig. 1 presents a normal empty stomach[2]. Note the folds called rugae. The cropped image contains only a part of a single ruga. Orthographic SfS reconstructed two peaks, which were incompatible with the original image (on the right and lower sides of the orthographic reconstruction). Perspective SfS reconstructed the ruga including its curved part.

The next row of Fig. 1 shows the gastric fundus[3]. The cropped version of this image focuses on a cavity with folded walls. The orthographic Fast Marching method failed to recover the cavity. Only a small part of its reconstruction could be attributed to this cavity (top–right of the orthographic reconstruction). The orthographically recovered folds showed little match to the true ones. The perspective method presented high correspondence of both the cavity and its folds to the contents of the original image.

In the third row of Fig. 1 we reconstructed part of the gastric angulus[3]. The cropped image shows three folds, all of which were clearly recovered by the perspective Fast Marching method. The orthographic method produced a pyramid-like peak with no folds.

The fourth row exhibits the descending duodenum[3]. The cropped version contains three plicae circulares (folds typical of the small intestine). The orthographic method yielded two surfaces with a sharp edge between them, which did not appear in the original data. The perspective method, on the other hand, recovered the folds.

The image at the bottom row (Fig. 1) was taken in the colon ascendens[3]. We concentrated on three plicae semicircularis (typical folds of the large intestine; see the cropped image). Even though this image visually resembles that of the gastric angulus, bear in mind that each shows a different organ; the difference is significant from the medical point of view. The orthographic reconstruction produced horizontal and vertical folds which did not exist in the original image. Two of the main folds could difficultly be noticed in the reconstruction (center and top–right of the figure). Both of these folds suffered strong noise in the form of short vertical folds. In the perspective reconstruction, all three folds were prominent.

Even though both algorithms use the same numerical methodology, the perspective Fast Marching method appears to outrank the orthographic one. This suggests that the

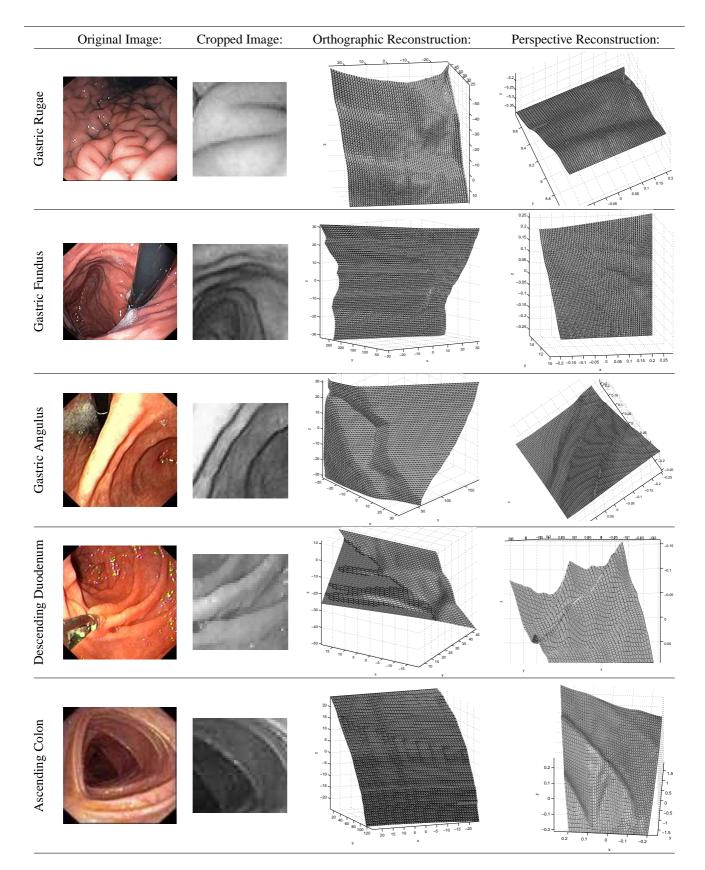|	Original Image:	Cropped Image:	Orthographic Reconstruction:	Perspective Reconstruction:
Gastric Rugae				
Gastric Fundus				
Gastric Angulus				
Descending Duodenum				
Ascending Colon				

Figure 1. Perspective vs. orthographic reconstruction of endoscopic images by the Fast Marching method. Images are of multiple parts of the gastrointestinal channel (as indicated to the left of each row).

assumption of a perspective rather than an orthographic image irradiance equation yields an important improvement in reconstruction.

While many orthographic algorithms rival the best numerical way to solve the classic equation, the suggested one adopts its numerical scheme from Kimmel and Sethian [7] and thus avoids competition in the numerical arena. Instead, it demonstrates that the perspective equation may be better suited for the task of SfS.

When comparing the perspective Fast Marching method with the perspective algorithm of [14], perspective Fast Marching has a prominent advantage of runtime. In [14], the famous synthetic Vase image without noise required about 1000 iterations to recover and about 2000 iterations when synthetic noise was added; a synthetic Mozart face image required about 4000 iterations (without noise). The suggested algorithm, on the other hand, needed only 2 iterations (1 orthographic initialization and 1 perspective iteration) to reconstruct real-life medical images. The computational complexity of an iteration of both algorithms ([14] and the suggested one) is $O(n)$ (where n is the number of image pixels), so a reduction of the number of iterations by three orders of magnitude is a significant improvement.

6. Conclusions

This research proposes an efficient and robust solution to the problem of Shape-from-Shading under the perspective projection model. The suggested solution employs a variant of the Fast Marching method of Kimmel and Sethian [7] to solve the perspective image irradiance equation of [20] and [14]. We compared reconstruction by the orthographic and perspective variants on medical images from various parts of the gastrointestinal tract (endoscopy). The perspective SfS algorithm outperforms the orthographic Fast Marching method. As we solved two models with a similar numerical scheme, the results must be related to the underlying assumptions, rather than to the numerical methodology. Consequently, we infer that the perspective assumption yields a significant improvement in reconstruction.

From the practical point of view, the comparison demonstrated that perspective SfS could be used for real-life images. The application to endoscopy suggests that, unlike orthographic SfS, perspective SfS is robust enough for real-life tasks.

The perspective Fast Marching method has a significant advantage over existing perspective methods ([20] and [14]) in terms of runtime. Only a single perspective iteration was required (in addition to the orthographic initialization) for reconstruction of all medical images tested.

Acknowledgements

A. Numerical Approximation and Its Solutions

A.1. The Equation

We bring the image irradiance equation to the form:

$$p^2 A + q^2 B + 2pqC + 2pD + 2qE + F_1 = 0$$

where:

$$
\begin{aligned}
A &\stackrel{\text{def}}{=} I^2 \|L\|^2 (u^2 + f^2) - (u - fp_s)^2 \\
B &\stackrel{\text{def}}{=} I^2 \|L\|^2 (v^2 + f^2) - (v - fq_s)^2 \\
C &\stackrel{\text{def}}{=} I^2 \|L\|^2 uv - (u - fp_s)(v - fq_s) \\
D &\stackrel{\text{def}}{=} I^2 \|L\|^2 u - (u - fp_s) \\
E &\stackrel{\text{def}}{=} I^2 \|L\|^2 v - (v - fq_s) \\
F_1 &\stackrel{\text{def}}{=} I^2 \|L\|^2 - 1
\end{aligned}
$$

We would like the left-hand side of this equation to be positive semidefinite. We therefore transfer non positive semidefinite terms to the right-hand side:

$$p^2 A_1 + q^2 B_1 = p^2 A_2 + q^2 B_2 - 2pqC - 2pD - 2qE - F_1$$

where:

$$
\begin{aligned}
A_1 &\stackrel{\text{def}}{=} I^2 \|L\|^2 (u^2 + f^2), & A_2 &\stackrel{\text{def}}{=} (u - fp_s)^2 \\
B_1 &\stackrel{\text{def}}{=} I^2 \|L\|^2 (v^2 + f^2), & B_2 &\stackrel{\text{def}}{=} (v - fq_s)^2
\end{aligned}
$$

Let us also define:

$$F \stackrel{\text{def}}{=} p^2 A_2 + q^2 B_2 - 2pqC - 2pD - 2qE - F_1$$

so the equation becomes:

$$p^2 A_1 + q^2 B_1 = F \tag{9}$$

where A_1 and B_1 are positive semidefinite, by definition. It therefore also implies: $F \geq 0$.

A.2. Solution of the Main Case

Similarly to [7], we assume W.L.O.G: $\Delta u = \Delta v = 1$, and estimate the directional derivatives by:

$$p_{ij} \approx z_{ij} - z_1, \quad q_{ij} \approx z_{ij} - z_2$$

where the notation is as described in Sect. 4.1. Substituting into Eq. 9, we get: $A_1(z_{ij} - z_1)^2 + B_1(z_{ij} - z_2)^2 = F_{ij}$, where $F_{ij} \stackrel{\text{def}}{=} F(i\Delta u, j\Delta v)$. Solving this equation for z_{ij} yields:

$$z_{ij} = \frac{A_1 z_1 + B_1 z_2 \pm \sqrt{(A_1 + B_1)F_{ij} - A_1 B_1 (z_1 - z_2)^2}}{A_1 + B_1} \tag{10}$$

A.3. Solution of the Degenerate Cases

The solution (Eq. 10) is degenerate when $\Delta \stackrel{\text{def}}{=} (A_1 + B_1)F_{ij} - A_1 B_1 (z_1 - z_2)^2 < 0$. Expressed differently,

$$|z_1 - z_2| > \sqrt{\frac{F_{ij}}{A_1} + \frac{F_{ij}}{B_1}} \qquad (11)$$

The next three lemmas solve Eq. 9 in the degenerate case. Their proofs are omitted for brevity.

Lemma 1 *If* $z_2 - z_1 > \sqrt{\frac{F_{ij}}{A_1}}$, *then* $z_{ij} \stackrel{\text{def}}{=} z_1 + \sqrt{\frac{F_{ij}}{A_1}}$ *is a solution of the equation:*

$$\begin{aligned}
\left(\max\{D_{ij}^{-u}z, -D_{ij}^{+u}z, 0\}\right)^2 A_1 + \\
\left(\max\{D_{ij}^{-v}z, -D_{ij}^{+v}z, 0\}\right)^2 B_1 = \quad F_{ij} \qquad (12)
\end{aligned}$$

Lemma 2 *If* $z_1 - z_2 > \sqrt{\frac{F_{ij}}{B_1}}$, *then* $z_{ij} \stackrel{\text{def}}{=} z_2 + \sqrt{\frac{F_{ij}}{B_1}}$ *is a solution of Eq. 12.*

Lemma 3 *If* $\Delta < 0$ *then necessarily either* $z_2 - z_1 > \sqrt{\frac{F_{ij}}{A_1}}$ *or* $z_1 - z_2 > \sqrt{\frac{F_{ij}}{B_1}}$ *holds. In other words, any degenerate case is contained in one of the cases of Lemmas 1 or 2.*

Lemmas 1 and 2 found solutions for the cases $z_2 - z_1 > \sqrt{\frac{F_{ij}}{A_1}}$ and $z_1 - z_2 > \sqrt{\frac{F_{ij}}{B_1}}$, respectively. Lemma 3 showed that these cases contain the degenerate case ($\Delta < 0$). Therefore, the solutions introduced by Lemmas 1 and 2 cover the degenerate case $\Delta < 0$.

References

[1] M. Bichsel and A. P. Pentland. A simple algorithm for shape from shading. In *CVPR*, pages 459–465, 1992.

[2] A. M. Bruckstein. On shape from shading. *Computer Vision, Graphics and Image Processing*, 44:139–154, 1988.

[3] P. Dupuis and J. Oliensis. An optimal control formulation and related numerical methods for a problem in shape reconstruction. *Annals of Applied Probability*, 4(2):287–346, 1994.

[4] B. K. P. Horn. Image intensity understanding. *Artificial Intelligence*, 8(2):201–231, Apr. 1977.

[5] B. K. P. Horn. *Robot Vision*. The MIT Press, 1986.

[6] R. Kimmel and A. M. Bruckstein. Global shape from shading. *Computer Vision and Image Understanding*, 62(3):360–369, Nov. 1995.

[7] R. Kimmel and J. A. Sethian. Optimal algorithm for shape from shading and path planning. *Journal of Mathematical Imaging and Vision*, 14(3):237–244, 2001.

[8] C.-H. Lee and A. Rosenfeld. Improved methods of estimating shape from shading using the light source coordinate system. *Artificial Intelligence*, 26:125–143, 1985.

[9] K. M. Lee and C.-C. J. Kuo. Shape from shading with a linear triangular element surface model. *Pattern Analysis and Machine Intelligence*, 15(8):815–822, Aug. 1993.

[10] K. M. Lee and C.-C. J. Kuo. Shape from Shading with a Generalized Reflectance Map Model. *Computer Vision and Image Understanding*, 67(2):143–160, Aug. 1997.

[11] T. Okatani and K. Deguchi. Shape reconstruction from an endoscope image by shape from shading technique for a point light source at the projection center. *Computer Vision and Image Understanding*, 66(2):119–131, May 1997.

[12] M. A. Penna. A Shape from Shading Analysis for a Single Perspective Image of a Polyhedron. *Pattern Analysis and Machine Intelligence*, 11(6):545–554, Jun. 1989.

[13] A. P. Pentland. Local shading analysis. *Pattern Analysis and Machine Intelligence*, 6(2):170–187, Mar. 1984.

[14] E. Prados and O. Faugeras. Perspective shape from shading and viscosity solutions. In *Proc. of the Intl. Conference on Computer Vision*, volume 2, pages 826–831, Oct. 2003.

[15] E. Prados, O. Faugeras, and E. Rouy. Shape from shading and viscosity solutions. In *European Conference on Computer Vision*, volume II, pages 790–804, Copenhagen, Denmark, May 2002.

[16] A. Robles-Kelly and E. R. Hancock. Model acquisition using shape-from-shading. In F. J. Perales and E. R. Hancock, editors, *Intl. Workshop on Articulated Motion and Deformable Objects*, pages 43–55, Palma de Mallorca, Nov. 2002.

[17] E. Rouy and A. Tourin. A viscosity solutions approach to shape-from-shading. *SIAM Journal of Numerical Analysis*, 29(3):867–884, Jun. 1992.

[18] D. Samaras and D. Metaxas. Coupled Lighting Direction and Shape Estimation from Single Images. *Proc. of the International Conference on Computer Vision*, 2:868–874, 1999.

[19] I. Seong, S. Hideo, and O. Shinji. A Divide-and-conquer Strategy in Shape from Shading Problem. In *Computer Vision and Pattern Recognition*, pages 413–419, 1997.

[20] A. Tankus, N. Sochen, and Y. Yeshurun. A new perspective [on] Shape-from-Shading. In *Proceedings of the 9th IEEE International Conference on Computer Vision*, volume II, pages 862–869, Nice, France, Oct. 2003.

[21] P.-S. Tsai and M. Shah. Shape from shading using linear approximation. *Image and Vision Computing*, 12(8):487–498, Oct. 1994.

[22] S. M. Yamany, A. A. Farag, E. Rickard, D. Tasman, and A. G. Farman. A Robust 3-d Reconstruction System for Human Jaw Modeling. In *Intl. Conf. on Medical Image Comp. and Computer-Assisted Intervention*, pages 778–787, 1999.

[23] S. Y. Yuen, Y. Y. Tsui, Y. W. Leung, and R. M. M. Chen. Fast marching method for shape from shading under perspective projection. In *Proc. of the IASTED International Conference on Visualization, Imaging, and Image Processing*, pages 584–589, Malaga, Spain, 2002.

[24] R. Zhang, P.-S. Tsai, J. E. Cryer, and M. Shah. Shape from shading: A survey. *Pattern Analysis and Machine Intelligence*, 21(8):690–705, Aug. 1999.

[25] W. Zhao and R. Chellappa. Face recognition using symmetric shape from shading. In *Proceedings of the IEEE Conference on Computer Vision and Pattern Recognition*, volume 4, pages 286–293, Hilton Head, SC, Jun. 2000.

[26] Q. Zheng and R. Chellappa. Estimation of illuminant direction, albedo, and shape from shading. *Pattern Analysis and Machine Intelligence*, 13(7):680–702, Jul. 1991.